Molecular-dynamics simulation of electron-ion recombination in a nonequilibrium, weakly ionized plasma

Wm. Lowell Morgan

Lawrence Livermore National Laboratory, University of California, Livermore, California 94550

(Received 9 February 1984)

Electron-ion recombination in a weakly ionized molecular gas has been studied by the application of molecular-dynamics and Monte Carlo simulations. Plasma screening effects have been investigated for electron densities exceeding 10^{13} cm^{-3}. Screening can reduce the recombination rate coefficient α by as much as one half, for $n_e = 10^{15}$ cm^{-3}, before α increases again with n_e due to electron-stabilized three-body collisional radiative recombination. In a plasma with an applied electric field, α is found to decrease approximately proportional to $(E/N)^{-1}$ for E/N greater than a threshold value.

I. INTRODUCTION

Recent experimental[1-3] and theoretical[4-8] research on electron-ion recombination has shown that, in the presence of a dense ambient molecular gas, rate coefficients approaching 10^{-4} cm^3/sec are feasible. This is due to enhancement of the recombination rate by inelastic collisions between the recombining electron and the ambient molecules. What constitutes a dense gas depends on the nature of the molecule. For instance, for H_2O, Warman et al.[1] have measured at 294 K and a density of 6.6×10^{17} cm^{-3} a recombination rate coefficient of 2.2×10^{-5} cm^3/sec that increases linearly with density. Calculations by Morgan[8] show that the rate coefficient can be expected to peak at about 1.3×10^{19} cm^{-3} with a value of approximately 7×10^{-5} cm^3/sec. These rate coefficients reach a peak with increasing pressure and then decline as particle transport in the dense gas becomes the rate-limiting step in recombination. Recombination in NH_3 behaves similarly[3,7] reaching its peak value at a pressure near 1 atm at 300 K. In both of these gases recombination is enhanced by the large electron collision frequency due to the dipole rotational cross sections at nearly thermal energy. In CO_2 the rate coefficient reaches a peak value[3,7] of approximately 10^{-4} cm^3/sec at about 8 atm pressure, and in CH_4 the peak rate[7] is about 8×10^{-5} cm/sec at 200 atm. Vibrational excitation processes enhance recombination in these gases. In this paper the phrase "low pressure" will refer to the pressure range below the peak where the rate coefficient α, is proportional to pressure P. Similarly, the phrase "high pressure" will refer to the pressure range above the peak, where α is inversely proportional to P.

During the recombination process an electron is accelerated toward a positive ion by their mutual Coulombic attraction, gaining enough energy to excite the rotational or vibrational modes of the ambient molecular gas, so that in a single collision it can lose a large fraction of its kinetic energy. If the electron is close enough to the ion that its total energy becomes negative by several kT or more upon colliding with a neutral molecule, then it can be considered to have recombined. We will call this three-body recombination and denote the rate coefficient for this process by α_3. In the monatomic gases, where the electron loses energy by elastic collisions only, the recombination rate coefficient is several orders of magnitude lower than the values quoted above.[9,10]

If the positive ion is a molecule that can undergo dissociative recombination then this becomes a competing channel with three-body recombination. The rate coefficient for this ostensibly two-body process is denoted by α_2. It has been suggested by Bates[5] that the presence of an ambient gas enhances dissociative recombination, in much the same manner as in ion-ion mutual neutralization,[11-13] so that α_2 is not equal to α_2^0, the zero-pressure dissociative recombination rate coefficient. Hence, the total rate coefficient $\alpha = \alpha_2 + \alpha_3 \neq \alpha_2^0 + \alpha_3$. The Monte Carlo simulations[7,8] of electron recombination have shown such an enhancement using an absorbing sphere model for dissociative recombination. Details are given in Ref. 7. At low pressure α increases with pressure as collisions are increasingly effective in promoting both two- and three-body recombination. At high pressure α is limited by the rate of approach of electrons and ions and decreases as P^{-1}.

Studies of recombination in weakly ionized plasmas have been pursued by numerous researchers for the whole of this century. An early measurement of α, the recombination rate coefficient, was performed by Thomson and Rutherford[14] in 1896. Early theories, which are still very useful today, were presented by Langevin[15] and by Thomson[16] for the high- and low-pressure limits, respectively. An excellent review of recombination theories has been written by Flannery.[17] Until relatively recent times the plasmas of interest were low pressure ($P < 10$ Torr) and very weakly ionized ($N_e < 10^{10}$ cm^{-3}) gas discharges. The development of lasers[18] and of discharge switches[19,20] has raised the pressure of interest to atmospheres and the electron and ion densities to $10^{13} - 10^{15}$ cm^{-3} or greater. At such pressures the three-body effects on recombination, as discussed above, become important. In addition, at such plasma densities Debye-Hückel screening may affect the recombination process. The effects of such screening on ion-ion recombination rates in a plasma environment have been investigated by numerical simulation by Morgan

et al.[21,22] and theoretically by Bates.[23] In this paper the molecular-dynamics method of simulating a system of many interacting particles is used to investigate electron-ion recombination in a weakly ionized plasma. The effects of plasma density and ambient gas pressure are investigated. In addition, the problem of recombination in the presence of an electric field, such as in the positive column of an electric discharge, is studied.

II. METHODS OF SIMULATING RECOMBINATION

Past numerical studies of ion-ion recombination have been made using Monte Carlo[21,24,25] (MC) simulations and molecular-dynamics[22] (MD) simulations. Recently, as mentioned above, the MC method has been applied to electron-ion recombination[7,8] and in this paper the MD method is used to investigate aspects of the problem not amenable to a two-particle simulation.

The MC simulations treat only a two-particle interaction within a boundary and use transport theory to establish boundary conditions. The MD method, on the other hand, includes collective effects (many-particle interactions) and avoids the *ad hoc* use of transport theory to connect microscopic and macroscopic physics. Hence such phenomena as plasma screening and non-Maxwellian particle distributions can be directly studied by the MD simulation. A description of each similation technique follows.

A. Monte Carlo simulation

The recombination process can be modeled[17] by treating the positive ion as a stationary sink toward which electrons diffuse due to both the Coulombic attraction and the density gradient set up around the sink by recombination. The principles involved in modeling this process by MC techniques are described in Refs. 24 and 25. The procedure involves two calculations: (1) the calculation, using a MC simulation, of the recombination probability for two ions starting at a distance r_0 apart with speeds selected from a thermal distribution and interacting through some force law; and (2) the calculation, using Fick's law, of the flux of ions crossing the surface of the sphere of diameter r_0 from $r > r_0$. This flux is given by

$$j(r) = -D\frac{dn_e(r)}{dr} + \mu_e e n_e(r)\frac{d\phi(r)}{dr} , \quad (1)$$

where D is the diffusion coefficient, μ_e is the mobility, and $\phi(r)$ is the average electric potential at a distance r from the positive ion. The first term in (1) describes the diffusion down the density gradient in the vicinity of the sink and the second term describes the electron drift in the electron field of the ion.

In these simulations the motion of the ions is neglected and the electrons are assumed to follow Coulomb trajectories between collisions. For each collision a set of random numbers is generated to determine the time at which the collision occurs, the state of the neutral molecule involved in the collision, and the change in energy and direction of the scattered electron. These determinations are simplified by use of the null-collision method,[26] which

involves the use of fictitious null collisions in which the velocity of the electron is unchanged. The cross section for these events is chosen to make the total collision rate independent of velocity, yielding a constant collision frequency. In this way momentum-transfer, rotational, and vibrational processes are included in the calculations.

In the application of MC to electron recombination, dissociative recombination of a molecular ion is modeled by the introduction of an absorbing sphere around the positive ion. The radius of this sphere is chosen so that the simulation yields the experimentally measured dissociative recombination rate coefficient α_2^0 at zero pressure.

The MC simulations are performed by starting the electron in each experiment a distance r_0 from the positive ion and following each trajectory, as described above. An experiment is terminated if (i) separation r_0 is again exceeded, (ii) the electron passes within the absorbing sphere, or (iii) the relative energy of the electron and ion becomes less than $-12kT$. Case (ii) is what we normally call two-body recombination and (iii) is called three-body recombination. Their rate coefficients are denoted by α_2 and α_3, respectively. More details on the MC simulation of charged-particle recombination are given in Refs. 7 and 25.

B. Molecular-dynamics simulation

A comprehensive review of the method of molecular dynamics has been written by Kushick and Berne.[27] Briefly, the classical equations of motion of a number of particles in a unit cell with periodic boundary conditions are integrated in time. Nearest images[28] of the particles are used in the calculation of interparticle forces. For the integration of equations of motion for the system of ions we have used the algorithm of Scofield:[29]

$$r(t+dt) = r(t) + v(t)dt + [4a(t) - a(t-dt)]dt^2/6 ,$$

$$v(t+dt) = v(t) + [2a(t+dt) + 5a(t) - a(t-dt)]dt/6 .$$

As described above, the null-collision method allows a constant time step to be used while accurately simulating inelastic and superelastic collisions between electrons and neutral molecules. We need only follow the ions and electrons in the calculation and not the neutral particles. This simulation represents a constant (T,V,N) canonical ensemble in that the neutral atoms function as a thermal reservoir which maintains a constant temperature. Additionally, as ions disappear from the volume due to recombination, new ion pairs are created in the unit cell with uniform spatial distribution and random Maxwellian thermal velocities. Hence the ion density is held constant in time. The molecular-dynamics simulation gives us a means of studying steady-state but nonequilibrium processes.

During the course of the MD simulation a variety of quantities are computed. The radial distribution function or pair correlation function $g(r)$ is obtained directly by counting the number of ion pairs with separation close to r. Diffusion coefficients for the positive and negative ions in the neutral gas can be computed from the mean-square displacement of the ions as a function of time.[30] If

there is an applied electric field a drift velocity in the direction of the field can also be calculated. Finally, the particle velocity distributions can be obtained by appropriate sampling.

These molecular-dynamics simulations of electron-ion recombination use 100 charged particles (50 of each type) in a cubic cell with sides of length 32 314 a_0, 15 000a_0, and 6962a_0 corresponding to ion densities of $n_e = n_i$ $= 10^{13}$, 10^{14}, and 10^{15} cm^{-3}, respectively. A typical time step used in this simulation is approximately 1000τ_0, where $\tau_0 = 2.42 \times 10^{-17}$ sec is the atomic unit of time. The time step used in these calculations is determined by the electron—neutral-molecule collision frequency. This is, typically, at least several orders of magnitude faster than the frequency of recombination. Because recombination is a relatively infrequent event, a great number of time steps are required for any reasonable statistical accuracy, with low electron density and high pressure representing the most severe case. In the calculations described below, for example, the number of time steps used ranges from 3×10^4 to 2×10^5 for $n_i = 10^{13}$ cm^{-3}.

If an electron and ion approach to within a distance r_0 of each other, the integration is stopped and the two-particle MC simulation described above is performed to determine if recombination takes place. This is done because the MD integration algorithm cannot accurately compute the trajectory of a rapidly moving electron in an orbit very near a positive ion. It is assumed that the two-body interaction, for which the trajectory can be described analytically, is dominant for small r_0 (500a_0 in these calculations). We see then that the *ad hoc* application of Fick's law to determine the flux of electrons and ions toward each other is eliminated and the charged-particle transport is simulated by MD.

III. RESULTS

A. Recombination in CO_2

1. Low pressure

Molecular-dynamics simulations have been performed for electrons and ions in CO_2 and in CH_4. The results of the CO_2 calculations are shown in Fig. 1 along with the total recombination rate coefficient calculated by Morgan and Bardsley[7] and that measured by Armstrong *et al.*[3] The cross-section data of Hake and Phelps[31] for elastic collisions and vibrational excitation have been used in these calculations. Looking first at the lower-pressure MD calculation we see that plasma screening reduces α by approximately a factor of 2 as the electron and ion densities are increased from 10^{13} to 10^{15} cm^{-3}. The Debye lengths corresponding to the three densities shown are at 300 K, 5050a_0, 1600a_0, and 505a_0.

More direct evidence of screening can be seen in Fig. 2 which shows the computed radial distribution functions for electron densities of 10^{13} and 10^{15} cm^{-3}. The radial distribution function (RDF) or ion-pair correlation function is defined as

$$g(r) \equiv n(r)/n_e , \tag{2}$$
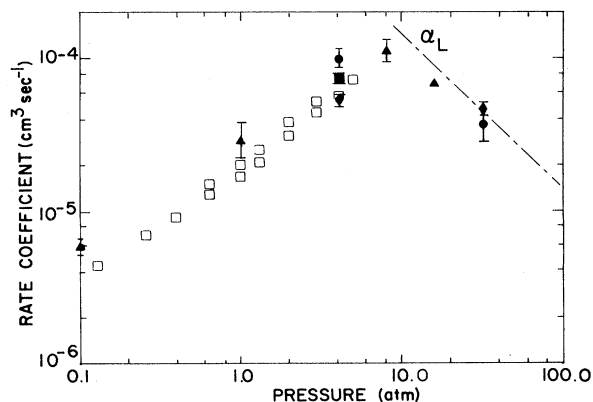
FIG. 1. Total recombination rate coefficient vs pressure for electrons in CO_2 at 300 K. The symobls ▲ are the Monte Carlo results from Ref. 7 and ●, ■, ◆ are the present molecular-dynamics results for $n_e = 10^{13}$, 10^{14}, 10^{15} cm^{-3}, respectively. The open symbols □ represent the experimental data of Ref. 3. The line —·— is the Langevin rate coefficient $\alpha_L = 4\pi e \mu_e$.

where $n(r)$ is the number density of electrons a distance r from a positive ion and $n_e = n(r = \infty)$ is the average electron density. For a plasma in local thermodynamic equilibrium (LTE) at temperature T with a Debye length

$$\lambda_D = \left[\frac{4\pi e^2}{kT} (n_i + n_e) \right]^{-1/2} , \tag{3}$$

the RDF is given by

$$g(r) = \exp(e^{-r/\lambda_D} e^2/rkT) . \tag{4}$$

The RDF's for $\lambda_D = \infty$, 5050A_0, and 505A_0 are shown as the smooth curves in Fig. 2. The Debye-Hückel screening is seen to reduce the ion-electron correlation distance as
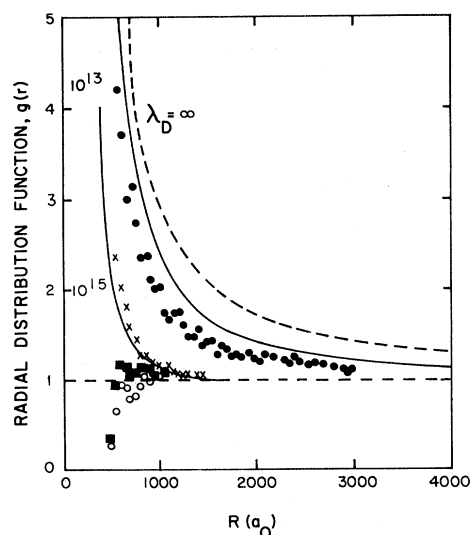
FIG. 2. Radial distribution functions for electron-ion pairs in CO_2. The dashed curve and the solid curves are $g(r)$ for $n_e = 0$, 10^{13}, and 10^{15} cm^{-3}. The calculated points are ●, $n_e = 10^{13}$, $p = 4$ atm; ×, $n_e = 10^{15}$, $p = 4$ atm; ○, $n_e = 10^{13}$, $p = 32$ atm; ■, $n_e = 10^{15}$, $p = 32$ atm.

λ_D becomes smaller. We see that the RDF's computed for electron densities of 10^{13} and 10^{15} cm^{-3} and a CO_2 pressure of 4 atm show approximately the same degree of plasma screening as the Debye-Hückel results.

2. High pressure

The MD results for recombination at a pressure of 32 atm, where the rate is limited by electron mobility, are shown in Fig. 1. Here we see that the rate coefficient for $n_e = 10^{15}$ cm^{-3} exceeds that of the lower electron density. Although the statistics are not very good, the radial distribution functions in Fig. 2 show evidence of this also. As had been found in the previous study of ion-ion recombination in a plasma,[22] $g(r)$ is less than unity and becomes smaller as $r \rightarrow r_0$. The effect of raising the plasma density is to decrease the average separation between charged particles and move $g(r)$ toward unity, thus increasing the correlation function in the neighborhood of r_0. This, of course, leads to an increase in the recombination rate. The increase, however, is small so that the Langevin formula,[15,32] $\alpha_L = 4\pi e \mu_e$, for the mobility (μ_e) limited rate coefficient is fairly accurate.

B. Recombination in CH$_4$

Several calculations of the recombination rate coefficient in methane are shown in Fig. 3. The Monte Carlo results shown are revisions of the calculations presented in Ref. 7, for which the excitation energy of the lowest vibrational mode of CH_4 was in error in the program. Using the correct energy, 0.17 eV, and the same calculational procedure and cross-section data[33] as described in Ref. 7, the two-body (α_2) and three-body (α_3) rate coefficients have been computed. The values of α shown are several times larger than those reported in Ref. 7. Note, though, that α is still smaller than the CO_2 recombination rates. The rate coefficient is not enhanced as much in CH_4 as in CO_2 because the excitation energy is higher. Of interest in this discussion, however, is the effect of plasma density upon α. These calculations, performed using molecular dynamics, are also shown in Fig. 3. At 1 atm we see that

the rate coefficient decreases slightly when n_e is increased from 10^{13} to 10^{14} cm^{-3}, but then for $n_e = 10^{15}$ cm^{-3}, α is substantially greater than that for 10^{13} cm^{-3}. The recombination rate due to collisions of the electron with neutral molecules,

$$e + CH_4^+ + CH_4 \rightarrow \text{products} ,$$

is small enough that recombination is now stabilized by electrons, i.e.,

$$e + CH_4^+ + e \rightarrow \text{products} .$$
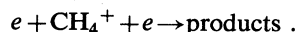
The rate coefficient for this process, known as collisional radiative recombination, is[34,35]

$$\alpha_{CRR} = 3.8 \times 10^{-9} T^{-9/2} n_e$$

which equals 2.71×10^{-5} cm^3/sec for $n_e = 1 \times 10^{15}$ cm^{-3} and $T = 300$ K. This lies within the uncertainty limits of the MD calculation. Bates[36] has pointed out in a discussion of ion-ion recombination in plasmas that a reduction of α due to plasma screening would, at some ion density, be masked by reactions having other ions as third bodies. This is just what we see here.

C. Remarks on nonequilibrium effects

Looking at the computed $g(r)$ for $P = 4$ atm in Fig. 2 we can see another effect. The computed and theoretical RDF agree well for $n_e = 10^{15}$ cm^{-3} but not nearly so well for the small electron density, $n_e = 10^{13}$ cm^{-3} and for r small compared to the average electron-ion separations. This is due to the non-LTE nature of this problem. At the higher electron density the electron-energy distribution function $f(\epsilon)$ is nearly a Maxwellian, whereas at the lower density it is not. This can be seen in Fig. 4 which plots $f(\epsilon)$, obtained by sampling electrons at a radius $r = 500a_0$ from positive ions, versus energy ϵ for two electron densities of interest. Here $f(\epsilon)$ is defined such that

$$\int_0^\infty f(\epsilon) \epsilon^{1/2} d\epsilon = 1 .$$

On the semilogarithmic graph a Maxwellian distribution,

FIG. 3. Total recombination rate coefficient vs pressure for electrons in CH_4 at 300 K. The shaded symbols are Monte Carlo results: ■, α_2; ●, α_3; and ▲, $\alpha = \alpha_2 + \alpha_3$. The open symbols are molecular-dynamics calculations of α for $n_e = 10^{13}$ cm^{-3} (○), 10^{14} cm^{-3} (□), and 10^{15} cm^{-3} (◇).
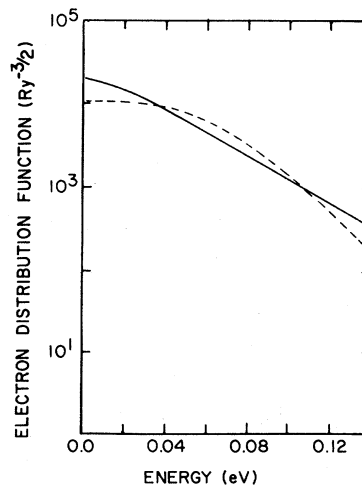
FIG. 4. The electron-energy distribution function vs energy at $r = 500a_0$ from a positive ion. The dashed curve — — — is for $n_e = 10^{13}$ cm^{-3} and the solid curve ——— is for $n_e = 10^{15}$ cm^{-3}.

$f(\epsilon) \propto \exp(-\epsilon/kT) = \exp(-mv^2/2kT)$, is a straight line. We see that $f(\epsilon)$ is nearly Maxwellian for $n_e = 10^{15}$ cm^{-3} but is quite non-Maxwellian for $n_e = 10^{13}$ cm^{-3}. This effect is well known[37,38] and is due to the removal of electrons from the tail of the distribution by inelastic collisions with the vibrational modes of CO_2. In the presence of an externally applied electric field even the bulk of the electrons, which are far from positive ions, are non-Maxwellian. As the electron density is increased $f(\epsilon)$ approaches a Maxwellian due to the thermalizing effects of electron-electron collisions.

For a system in LTE the Boltzmann equation has as a solution[39] the distribution function

$$f(\vec{r},\vec{v}) = f_0(\vec{v})e^{-\phi(\vec{r})/kT}$$

for a conservative force given by $\vec{F} = -\vec{\nabla}\phi(\vec{r})$. The velocity distribution function is the usual Maxwellian. Now $\phi(\vec{r})$, the potential of mean force,[40] is related to the radial distribution function by just the relation

$$g(\vec{r}) = e^{-\phi(\vec{r})/kT} . \tag{5}$$

The charge density at $\vec{r}$ is $\rho(\vec{r}) = n_e g(\vec{r})$. Poisson's equation is solved using this $\rho(\vec{r})$ and the linearization $g(\vec{r}) \simeq 1 - \phi(\vec{r})/kT$. The Debye-Hückel RDF, Eq. (4), is then obtained along with the definition, Eq. (3), of the Debye length. The separation of the solution $f(\vec{r},\vec{v})$ of the Boltzmann equation into a simple product $f_0(\vec{v})g(\vec{r})$ depends upon $f_0(\vec{v})$ being Maxwellian. If $f_0(\vec{v})$ is not Maxwellian the problem becomes substantially more complicated and $g(\vec{r})$ is, in general, not given by (4). A detailed discussion of the expansion of the distribution function and solution of the Boltzmann equation in nonequilibrium, weakly ionized plasmas is given by Kumar et al.[41]

We see from the foregoing that just as temperature is not a well-defined quantity for non-Maxwellian distributions, the Debye length itself is not well defined. More general definitions and formulations are needed for the steady state, non-LTE problem. The general formulation of nonequilibrium plasma physics[42] involves the dynamic structure factor $S(\vec{k},\omega)$ defined by

$$S(\vec{k},\omega) = \frac{1}{|\epsilon(\vec{k},\omega)|^2} \int_0^\infty d\vec{v}\, f(\vec{v})\delta(\omega - \vec{k}\cdot\vec{v}) , \tag{6a}$$

where $\epsilon(\vec{k},\omega)$ is the dielectric response function

$$\epsilon(\vec{k},\omega) = 1 + \frac{\omega_p^2}{k^2}\int_0^\infty d\vec{v}\, \frac{1}{\omega - \vec{k}\cdot\vec{v}}\vec{k}\cdot\frac{\partial}{\partial\vec{v}}f(\vec{v}) . \tag{6b}$$

In (6b), ω_p is the plasma frequency. Now the electron velocity distribution and the radial distribution function are related, in a more general sense, through the static structure factor $S(\vec{k})$ by

$$S(|\vec{k}|) = 1 + n_e \int_0^\infty \exp(i\vec{k}\cdot\vec{r})g(\vec{r})d\vec{r} = \int_{-\infty}^{+\infty} S(\vec{k},\omega)d\omega . \tag{7}$$

This is the formalism that relates the nonequilibrium velocity distribution and pair correlation function without appealing to equilbrium concepts such as temperature and Debye length.

Non-Maxwellian distributions, it should be noted, may have observable effects on spectral line profiles.[43-45] These are related to the local electric field by

$$I(\omega) = \int P(E)J(\omega,E)dE , \tag{8}$$

where $P(E)$ is the microfield distribution and $J(\omega,E)$ is a profile function containing all the dynamic perturbations. $J(\omega,E)$ is a function of the dynamic structure factor $S(\vec{k},\omega)$ defined by Eqs. (6a) and (6b). We see that the structure factor is a fundamental function defining the relationships among a variety of plasma properties.

IV. RECOMBINATION IN A DISCHARGE

As mentioned in the Introduction, we can use the molecular-dynamics method to simulate recombination in a discharge, i.e., with an externally applied electric field. Such calculations have been performed for recombination in CO_2, and in CH_4. The results of both sets of calculations for an electron density of 10^{14} cm^{-3} are shown in Fig. 5. In these simulations the electric field is included in the equations of motion only for the MD part of the calculation. In the MC simulation, performed for electrons and ions that are within a distance r_0 of each other, the usual central-force motion is assumed. The success of this approximation depends upon the Coulomb force between electron and ion being stronger than the external force for separations less than r_0. In a discharge E/N, the electric field divided by the total gas number density, is the parameter of importance. The criterion for the use of this approximation is then

$$\frac{1}{r_0^2 N} \gtrsim \frac{E}{N} .$$

The value of $1/(r_0^2 N)$ for a pressure of 1 atm at 300 K and $r_0 = 500a_0$ is 7.6×10^{-16} V cm^2. As a historical note, the classical mechanics problem of the effect of an external field on central-force motion has an analytic solution in parabolic coordinates and was the model for the hydrogen Stark effect in the era before quantum mechanics.[46,47] As an alternative to performing the Monte Carlo simulation in parabolic coordinates we have the option of reduc-
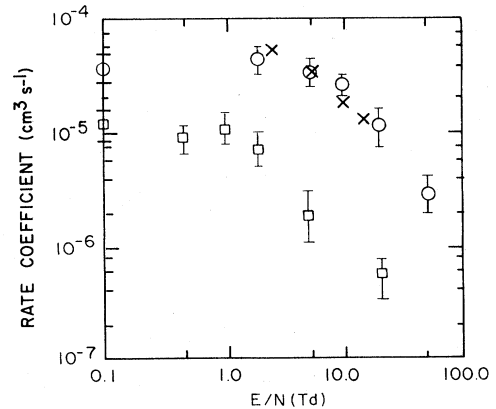
FIG. 5. Total rate coefficient for recombination of electrons and ions in a discharge as a function of E/N for CO_2 (O) and CH_4 (□). The experimental results for CO_2 of Ref. 49 are denoted by the symbol ×.

ing r_0 in order to satisfy the above criterion. For CO_2, test calculations varying r_0 were performed for the largest value of E/N shown and the computed α was found to vary within the error limits shown, although this is likely to be about the maximum E/N for which trustworthy results would be obtained.

Since the mean electron energy $(\bar{\epsilon})$, the diffusion coefficient (D), and the mobility (μ_e) can be computed as functions of E/N, some approximate proportionalities can be found between α and these quantities. An experimentally measurable quantity is the characteristic energy[48] D/μ_e which is frequently known even if the mean energy is not. For a Maxwellian electron distribution, $kT = \frac{2}{3}\bar{\epsilon} = D/\mu_e$. Electron-energy distributions in discharges, however, are usually non-Maxwellian.[32,33] Curves of drift velocity $(\mu_e E)$ and characteristic energy versus E/N for electrons in CO_2 and in CH_4 are given in Refs. 31 and 42, respectively. These data yield the following approximate dependencies for α in CH_4 at 1 atm:

$$\alpha \propto (E/N)^{-1} \propto (D/\mu_e)^{-0.77} \propto \bar{\epsilon}^{-1.2}$$

For CO_2, unlike CH_4, the curve of D/μ_e versus E/N does not have a simple power-law dependence over the range of E/N above 5 Td. So, we have only very approximately, for CO_2 at 1 atm,

$$\alpha \propto (E/N)^{-1} \propto (D/\mu_e)^{-0.45}.$$

In this E/N range the mean energy goes from approximately a quadradic E/N dependence to a linear dependence so that no simple relation between α and $\bar{\epsilon}$ can be found.

These calculations are in good agreement with the recent experimental measurements by Littlewood et al.[49] of the recombination rate of ions in CO_2 at near-atmospheric pressure. These data are also shown in Fig. 5. They also found that the pressure dependence of α diminishes with increasing E/N. In their experiments the three-body recombination rate declines precipitously with E/N while the two-body rate decreases more slowly. At the highest field strengths in the experiments, $13-20$ Td, α appears to have no pressure dependence up to 600 Torr. This is consistent with the model presented here. At high fields α_3 is very small and α_2 goes to the zero-pressure limit. This is because the two-body process is modeled by an ab-sorbing sphere of fixed radius. In reality, however, the zero-pressure dissociative recombination rate coefficient is temperature dependent and, thus, the absorbing-sphere model should have an energy-dependent cross section.

V. SUMMARY

The molecular-dynamics method has been used to simulate electron-ion recombination in a weakly ionized plasma. For low pressures of ambient neutral molecules, where $\alpha \propto P$, screening has been found to reduce the recombination rate by about a factor of 2 at most for electron densities of 10^{15} cm^{-3}. For molecules such as CH_4 that do not enhance the neutral-stabilized rate as much as does CO_2, the electron-stabilized collisional radiative rate becomes dominant. Clearly, for large enough n_e, electron-stabilized recombination will dominate in any molecular gas. In the high-pressure region, where $\alpha \propto 1/P$, the rate coefficient is found to increase with electron density although the effect is small; α actually deviates little from the Langevin mobility limit.

Recombination in an external field, such as in an electric discharge, has also been studied. The rate coefficient is found to decrease with applied field approximately proportional to $(E/N)^{-1}$, in good agreement with very recent experimental measurements.

The molecular-dynamics simulation is a robust method of studying the microscopic physics of such nonequilibrium systems as the weakly ionized plasmas discussed above. Much information can be obtained by simulating the particle dynamics and calculating transport coefficients, distribution functions, and correlation functions. Hopefully the method will, in the future, find wider application to other problems in gaseous electronics.

ACKNOWLEDGMENTS

[1]J. M. Warman, E. S. Sennhauser, and D. A. Armstrong, J. Chem. Phys. 70, 995 (1979).
[2]E. S. Sennhauser, D. A. Armstrong, and J. W. Warman, Radiat. Phys. Chem. 15, 479 (1980).
[3]D. A. Armstrong, E. S. Sennhauser, J. M. Warman, and V. Sowada, Chem. Phys. Lett. 86, 281 (1982).
[4]D. R. Bates, J. Phys. B 13, 2587 (1980).
[5]D. R. Bates, J. Phys. B 14, 3525 (1981).
[6]D. R. Bates, Chem. Phys. Lett. 89, 294 (1982).
[7]W. L. Morgan and J. N. Bardsley, Chem. Phys. Lett. 96, 93 (1983).
[8]W. L. Morgan, J. Chem. Phys. 80, 4564 (1984).
[9]D. R. Bates and S. P. Khare, Proc. R. Soc. London 85, 231 (1965).
[10]B. L. Whitten, L. W. Downes, and W. E. Wells, J. Appl. Phys.

52, 1255 (1981).
[11]D. R. Bates, J. Phys. B 14, 4207 (1981).
[12]B. L. Whitten, W. L. Morgan, and J. N. Bardsley, J. Phys. B 15, 319 (1982).
[13]D. R. Bates and W. L. Morgan, Chem. Phys. Lett. 101, 18 (1983).
[14]J. J. Thomson and E. Rutherford, Philos. Mag. 42, 392 (1896).
[15]P. Langevin, Ann. Chim. Phys. 28, 433 (1903).
[16]J. J. Thomson, Philos. Mag. 47, 337 (1924).
[17]M. R. Flannery, in Atomic Processes and Applications, edited by P. G. Burke and B. L. Moiseiwitsch (North-Holland, Amsterdam, 1976).
[18]J. D. Daugherty, in Principles of Laser Plasmas, edited by G. Bekefi (Wiley, New York, 1976).
[19]L. Kline, IEEE Trans. Plasma Sci. 10, 224 (1982).

[20]M. Kristiansen and A. H. Guenther, in *Electrical Breakdown and Discharges in Gases, Part B,* edited by E. E. Kunhardt and L. H. Luessen (Plenum, New York, 1983).

[21]W. L. Morgan, B. L. Whitten, and J. N. Bardsley, Phys. Rev. Lett. **45**, 2021 (1980).

[22]W. L. Morgan, J. N. Bardsley, J. Lin, and B. L. Whitten, Phys. Rev. A **26**, 1696 (1982).

[23]D. R. Bates, J. Phys. B **15**, L755 (1982).

[24]D. R. Bates and I. Mendaš, Proc. R. Soc. London, Ser. A **359**, 287 (1978).

[25]J. N. Bardsley and J. M. Wadehra, Chem. Phys. Lett. **72**, 477 (1980).

[26]S. L. Lin and J. N. Bardsley, Comput. Phys. Commun. **15**, 161 (1978).

[27]J. Kushick and B. J. Berne, in *Statistical Mechanics, Part B,* edited by B. H. Berne (Plenum, New York, 1977).

[28]W. W. Wood and F. R. Parker, J. Chem. Phys. **22**, 720 (1957).

[29]P. Scofield, Comput. Phys. Commun. **5**, 17 (1973).

[30]E. Helfand, Phys. Rev. **119**, 1 (1960).

[31]R. D. Hake and A. V. Phelps, Phys. Rev. **158**, 70 (1967).

[32]D. R. Bates, J. Phys. B **16**, L295 (1983).

[33]L. C. Pitchford, S. V. O'Neil, and J. R. Rumble, Jr., Phys. Rev. A **23**, 294 (1981).

[34]P. Mansbach and J. Keck, Phys. Rev. **181**, 275 (1967).

[35]J. Stevefelt, J. Boulmer, and J. F. Delpech, Phys. Rev. A **12**,

1246 (1975).

[36]D. R. Bates, J. Phys. B **15**, L755 (1982).

[37]W. L. Nighan, Phys. Rev. A **2**, 1989 (1970).

[38]L. C. Pitchford, in *Electrical Breakdown and Discharges in Gases, Part A,* edited by E. E. Kunhardt and L. H. Luessen (Plenum, New York, 1983).

[39]K. Huang, *Statistical Mechanics* (Wiley, New York, 1963).

[40]D. A. McQuarrie, *Statistical Mechanics* (Harper and Row, New York, 1975).

[41]K. Kumar, H. R. Skullerud, and R. E. Robson, Aust. J. Phys. **33**, 343 (1980).

[42]S. Ichimaru, *Basic Principles of Plasma Physics* (Benjamin, Reading, 1973).

[43]R. W. Lee, J. Phys. B **12**, 1165 (1979).

[44]W. R. Chappell, J. Cooper, and E. W. Smith, J. Quant. Spectrosc. Radiat. Transfer **10**, 1195 (1920).

[45]R. W. Lee and W. L. Morgan (unpublished).

[46]M. Born, *The Mechanics of the Atom* (Bell and Sons, London, 1927).

[47]R. W. Wood, Phys. Rev. **38**, 346 (1931).

[48]E. W. McDaniel, *Collision Phenomena in Ionized Gases* (Wiley, New York, 1964).

[49]I. Littlewood, M. C. Cornell, B. K. Clark, and K. J. Nygaard, J. Phys. D **16**, 2113 (1983).